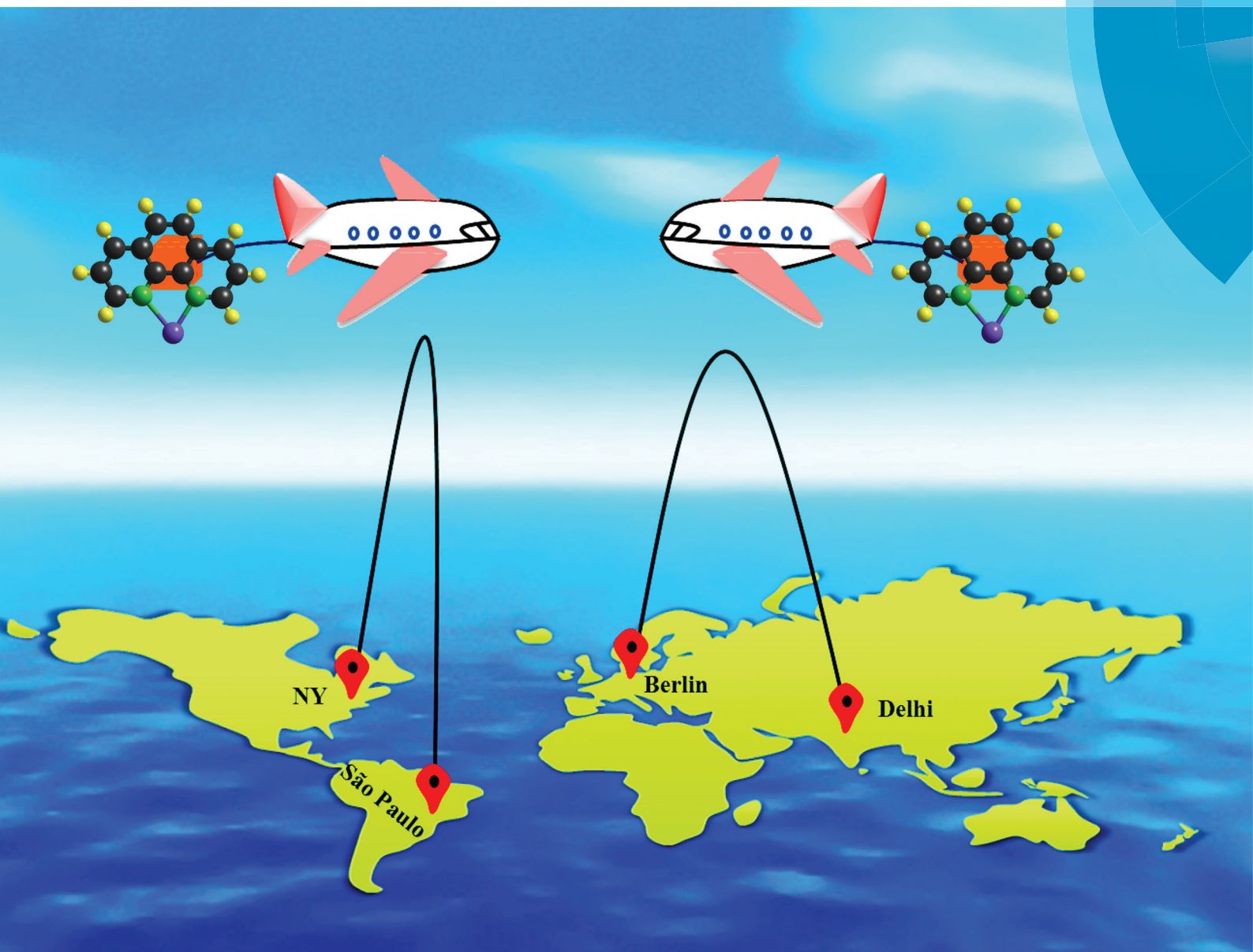


Dalton Transactions

An international journal of inorganic chemistry

www.rsc.org/dalton



ISSN 1477-9226



PAPER

Michael Schmittl *et al.*

Reversible cargo shipping between orthogonal stations of a nanoscaffold upon redox input

Reversible cargo shipping between orthogonal stations of a nanoscaffold upon redox input†

Soumen K. Samanta, Anup Rana and Michael Schmittel*

Cite this: *Dalton Trans.*, 2014, **43**, 9438Received 20th March 2014,
Accepted 6th May 2014

DOI: 10.1039/c4dt00849a

www.rsc.org/dalton

Introduction

Many enzymes use translocation processes¹ (ligand and metal) to initiate fascinating biological protocols. Likewise, shifting subcomponents in either supramolecular² or molecular³ structures has been ingeniously utilised in fascinating abiological devices.^{4,5} To control reversible motion in multistable devices by switching, the binding of the movable part (K_{assoc}) has to favour a particular site over the other depending on the given input, such as chemicals,⁶ redox equivalents⁷ or light.⁸

As reported by Sauvage and coworkers,⁹ changing the oxidation state of copper from +I to +II leads to an altered coordination preference: the copper(I) ion prefers tetracoordination, while the copper(II) ion is best accommodated in a penta- or hexacoordination. Remodeling this principle, we present here the reversible shipping of cargo between two different sites on a scaffold by applying electrochemical stimuli (Fig. 1). Our design of reversible cargo shipping relies on two heteroleptic binding algorithms developed in our group, *i.e.* the HETPHEN and HETTAP concepts,¹⁰ instead of using topological constraints, as is amply done in rotaxanes and catenanes.¹¹ Our concepts are based on the use of a bulky 2,9-diaryl substituted phenanthroline (PhenAr₂), *e.g.*, ligand **3** (Chart 1),¹² whose front-side shielding prevents the formation of the homoleptic

The sterically shielded terpyridine **5** was prepared, both as a new ligand and as part of the four-station nanoscaffold **2**. Mixing of terpyridine **5**, the parent phenanthroline **4** and the shielded phenanthroline **3** in the presence of Zn²⁺ (1 : 1 : 1) furnished quantitatively the inverse HETTAP complex [Zn(**4**)(**5**)]²⁺ by self-sorting, while in the presence of Cu⁺ the HETPHEN complex [Cu(**3**)(**4**)]⁺ was preferred (89%). Due to the akin coordination preferences of Cu²⁺ and Zn²⁺, the above self-sorting was implemented for Cu⁺/Cu²⁺ on nanoscaffold **2**, the latter equipped with the binding motifs of **3** (PhenAr₂) and **5** (TerpyAr₂). When **2** was reacted with Cu⁺ and phenanthroline (**4**) in a 1 : 2 : 2 ratio, only the PhenAr₂ stations became involved in complex formation (= ^{Cu}**1**_{phen}). In contrast, upon oxidative formation of Cu²⁺, ligand **4** was exclusively moved to the TerpyAr₂ stations (= ^{Cu}**1**_{terpy}). Electrochemical oxidation–reduction prompted the cargo to be shipped reversibly on a subsecond time scale between the two different stations of **2**.

complex [M(**3**)₂]ⁿ⁺ with Mⁿ⁺ = Cu⁺, Ag⁺, Zn²⁺. In presence of a sterically slim counterpart, like the parent phenanthroline (for HETPHEN)^{12a,b} or terpyridine (for HETTAP),^{12c,d} **3** and Mⁿ⁺ will afford quantitatively the heteroleptic complex.

For the present study, structural aspects known from the HETTAP and HETPHEN protocols guided our design of the new terpyridine **5** that is sterically shielded by aryl groups (TerpyAr₂). The shielding does not prevent, but slows down formation of the homoleptic complex [M(TerpyAr₂)₂]ⁿ⁺ thus favouring heteroleptic complexation. The new scaffold **2** arises by attaching the binding motifs of both PhenAr₂ and TerpyAr₂ sites to a zinc(II) porphyrin core. Depending on the oxidation state of the copper ions a switch in the self-sorting¹³ should lead to cargo shuffling (cargo = copper + ligand **4**) between the PhenAr₂ and TerpyAr₂ stations on the scaffold (Fig. 1). As such, our example is a very rare case of redox initiated self-sorting¹⁴ in solution.

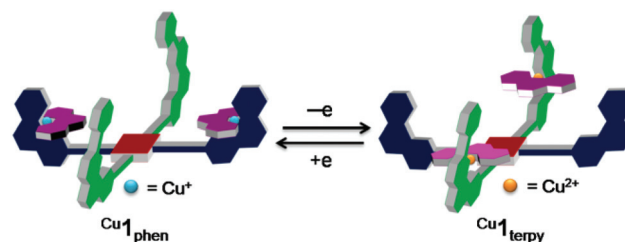


Fig. 1 Controlling cargo transport between two stations *via* self-sorting by oxidation/reduction. ^{Cu}**1**_{phen} = [Cu₂(**2**)(**4**)₂]²⁺. ^{Cu}**1**_{terpy} = [Cu₂(**2**)(**4**)₂]⁴⁺.

Center of Micro- and Nanochemistry and Engineering, Organische Chemie I,
Universität Siegen, Adolf-Reichwein-Str. 2, D-57068 Siegen, Germany.

E-mail: schmittel@chemie.uni-siegen.de

† Electronic supplementary information (ESI) available: ¹H, ¹H–¹H COSY, ¹³C NMR, ESI-MS, cyclic voltammograms, DOSY and DFT optimised structures. See DOI: 10.1039/c4dt00967c



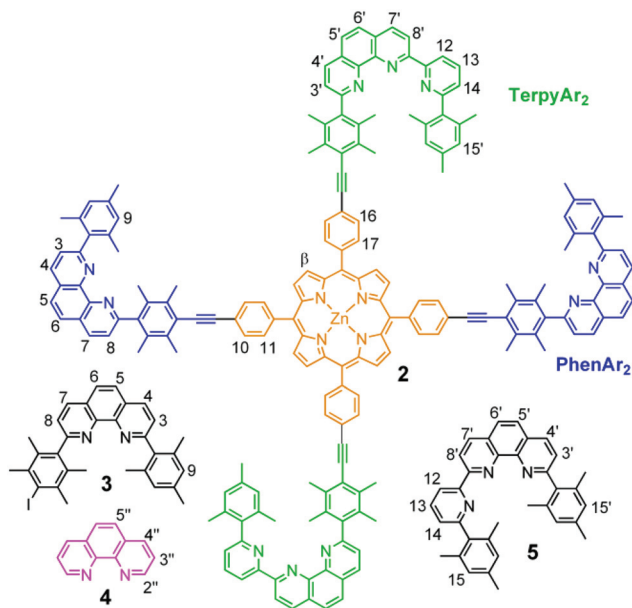


Chart 1 Scaffold 2 and ligands 3–5 used in the present study.

Results and discussion

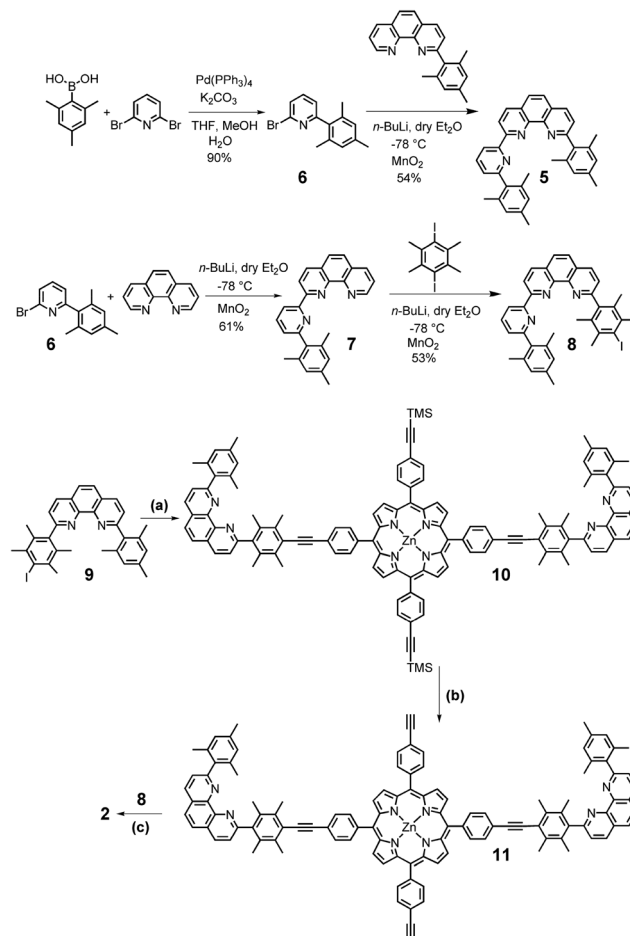
Synthesis

The new compounds 2 and 5 (Scheme 1) were prepared *via* established protocols. First, 2,4,6-trimethylphenylboronic acid was treated with 2,6-dibromopyridine *via* Suzuki coupling to furnish compound 6, which was reacted further on with 2-(2,4,6-trimethylphenyl)-[1,10]-phenanthroline to afford ligand 5.

For the preparation of scaffold 2 with two different kinds of stations, pyridine 6 was subjected to a bromo/lithium exchange and then reacted with [1,10]-phenanthroline to afford the terpyridine-analog 7. A follow-up reaction with 1,4-diiododurene/*n*-BuLi furnished 8 serving as the direct precursor for the preparation of scaffold 2. To finalise the synthesis, zinc(II)-5,15-bis(4-iodophenyl)-10,20-bis(4-trimethylsilylethynylphenyl)porphyrin was first treated with the known shielded phenanthroline **9**^{12d} in presence of Pd(PPh₃)₄ to afford 10, which after deprotection of the trimethylsilyl groups furnished 11. In the final step, 11 was reacted with ligand 8 in a second Sonogashira coupling to provide the desired target 2 (Scheme 1). Scaffold 2 was easily and fully characterised by spectroscopic means.

Complexation properties of 5

Insight into the binding properties of 5 was received by reacting 0.5 equiv. of [Cu(CH₃CN)₄]PF₆ with 5 in CD₂Cl₂. ¹H NMR and ESI-MS of the resulting yellow solution revealed formation of the homoleptic complex [Cu(5)₂]⁺ by showing two different sets of upfield shifted mesityl protons at 5.62 and 6.19 ppm (Fig. 2) and a mass peak at 1051.0 Da. Assuming a coordination number 4 for Cu⁺, [Cu(5)₂]⁺ may actually form in three isomeric structures, *i.e.* iso-I, iso-II & iso-III (Charts 2 and 3)



Scheme 1 Synthesis of ligands 2, 5 and 8. (a) Zinc(II)-5,15-bis(4-iodophenyl)-10,20-bis(4-trimethylsilylethynylphenyl)porphyrin, Pd(PPh₃)₄, NEt₃, DMF, 90 °C, 12 h, 58%. (b) KOH, THF, MeOH, room temperature, 90%. (c) Pd(PPh₃)₄, NEt₃, DMF, 90 °C, 12 h, 35%.

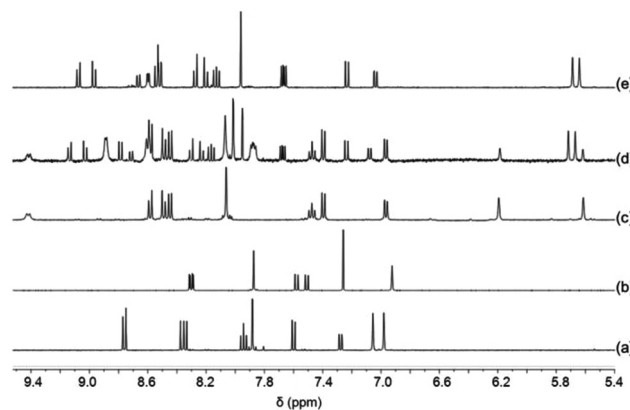


Fig. 2 Partial ¹H NMR spectra of (a) 5 in CD₂Cl₂, (b) 3 in CDCl₃, (c) [Cu(5)₂]⁺PF₆ in CD₂Cl₂, (d) equimolar mixture of 4, 5 and Cu⁺ in CD₂Cl₂ and (e) equimolar mixture of 4, 5 and Zn²⁺ (in CD₂Cl₂–CD₃CN = 3 : 1).

due to six nitrogen atoms being available from two ligands 5. In iso-I, Cu⁺ engages exclusively with the phenanthroline nitrogen atoms (N2, N3, N2' and N3'), while the pyridyl nitrogen



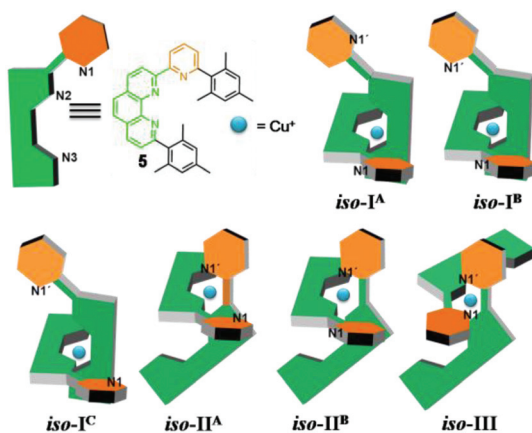


Chart 2 Cartoon representations of compound **5** and the three isomers (iso-I, iso-II & iso-III) of the homoleptic complex $[\text{Cu}(\text{5})_2]^+$. Superscript letters A, B and C denote conformations.

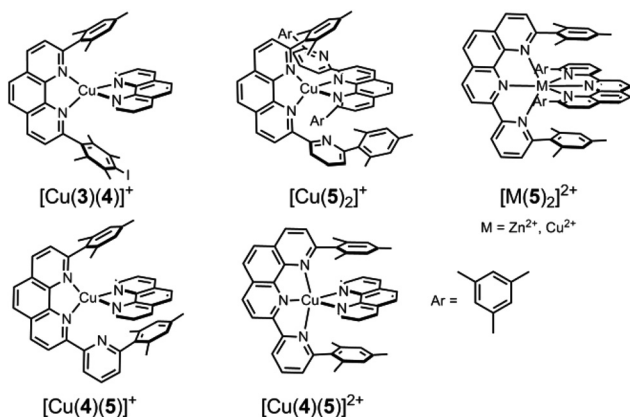


Chart 3 Possible complexes resulting from ligands **3**, **4**, **5** and the metal ions Cu^+ , Cu^{2+} and Zn^{2+} .

atoms (N1 and N1') remain unbound. In iso-II, Cu^+ is bound to N2, N3, N2', N1' whereas N1, N3' are left uncoordinated. In contrast, iso-III deals with coordination at N2, N1, N2', N1' with nitrogens N3, N3' remaining nonbonded. The unbound pyridyl unit (N1 or N1') of **5** may undergo rotation about the single C–C bond thereby generating various conformations in iso-I and iso-II of $[\text{Cu}(\text{5})_2]^+$. For instance, iso-I may have three major conformers – iso-I^A (*out-out* = N1 and N1' directed away from Cu^+ center), iso-I^B (*out-in*), and iso-I^C (*in-in*). Similarly iso-II may have two conformers – iso-II^A (*in*) and iso-II^B (*out*). Obviously, in iso-III both pyridyl units are conformationally fixed as they are involved in bonding with Cu^+ . DFT¹⁵ computations suggest that iso-I^B has lowest energy. The relative energy of the isomers follows the order: iso-I^B (0) < iso-I^A (3.94) < iso-II^B (4.04) < iso-II^A (6.62) kcal mol⁻¹.¹⁶

Experimental information about the coordination mode in $[\text{Cu}(\text{5})_2]^+$ was obtained from cyclic voltammetry (CV). Complex $[\text{Cu}(\text{5})_2]^+$ exhibits a high oxidation potential at $E_{1/2} = 634$ mV_{SCE} (quasireversible: $\Delta E_p = 164$ mV, see ESI[†]) clearly excluding the possibility of penta- or hexa-coordination. Most

likely, steric crowding by the mesityl groups prevents Cu^{2+} to extend its coordination number from 4 to 5/6.

Heteroleptic complexes with ligand **5**

When a 1 : 1 : 1 mixture of **4**, **5** and copper(i) ions was reacted in CD_2Cl_2 , the homoleptic complexes $[\text{Cu}(\text{4})_2]^+$ and $[\text{Cu}(\text{5})_2]^+$ as well as the heteroleptic complex $[\text{Cu}(\text{4})(\text{5})]^+$ were observed in the ESI-MS, with the latter generating the major peak (at 745.5 Da). The ¹H NMR data corroborate the formation of both complexes $[\text{Cu}(\text{4})(\text{5})]^+$ and $[\text{Cu}(\text{5})_2]^+$ (Fig. 2), with peaks at 5.63 & 5.69 ppm being diagnostic for $[\text{Cu}(\text{4})(\text{5})]^+$ and those at 5.62 and 6.19 ppm (Fig. 2) for $[\text{Cu}(\text{5})_2]^+$. Unfortunately, characteristic signals for $[\text{Cu}(\text{4})_2]^+$ were obscured in the aromatic region.

The DFT optimised structure of $[\text{Cu}(\text{4})(\text{5})]^+$ predicts that the metal ion is engaged in coordination with both phenanthroline nitrogens (N2 and N3) of **5**, while the pyridyl nitrogen atom (N1) remains nonbonded. Strong $\pi \cdots \pi$ interactions (C \cdots C = 4.033 Å and 4.043 Å) between the two mesityl units of **5** and **4** are observed. Other isomers of $[\text{Cu}(\text{4})(\text{5})]^+$ involving N1(pyridyl)→Cu interactions were not located computationally.

When an equimolar mixture of **4**, **5** and Cu(i) was oxidised in CV, a broad wave at 540–713 mV was observed corresponding to oxidation of all three copper complexes, $[\text{Cu}(\text{4})_2]^+$, $[\text{Cu}(\text{5})_2]^+$ and $[\text{Cu}(\text{4})(\text{5})]^+$. In contrast, the cathodic scan generated a single, irreversible peak at $E_{pc} = 251$ mV assigned to the reduction of $[\text{Cu}(\text{4})(\text{5})]^{2+}$ exclusively. Indeed, the independently prepared complex $[\text{Cu}(\text{4})(\text{5})]^{2+}$ (*vide infra*) showed a reduction wave at $E_{pc} = 245$ mV. Apparently, upon oxidation, both homoleptic complexes $[\text{Cu}(\text{5})_2]^{2+}$ and $[\text{Cu}(\text{4})_2]^{2+}$ reorganised to $[\text{Cu}(\text{4})(\text{5})]^{2+}$ so that each copper(ii) ion would realise pentacoordination in the heteroleptic complex.

When a 1 : 1 mixture of **4** and **5** was treated with 1 equiv. of $\text{Zn}(\text{OTf})_2$ in CD_2Cl_2 – $\text{CD}_3\text{CN} = 3 : 1$, the heteroleptic complex $[\text{Zn}(\text{4})(\text{5})]^{2+}$ formed quantitatively as documented by spectroscopic data. The ESI mass spectrum shows peaks at 370.0 Da and 888.3 Da diagnostic for the doubly charged $[\text{Zn}(\text{4})(\text{5})]^{2+}$ and singly charged $[\text{Zn}(\text{4})(\text{5})](\text{OTf})^+$ after loss of two and one counteranion(s) (OTf^-), respectively (Fig. S37, ESI[†]). No mass peaks of homoleptic complexes are visible. The ¹H NMR spectrum displays two diagnostic signals at 5.64 & 5.69 ppm for the heteroleptic species (Fig. 2).

Due to the similarity in its coordination behaviour to that of Zn^{2+} , Cu^{2+} also afforded cleanly the heteroleptic complex $[\text{Cu}(\text{4})(\text{5})]^{2+}$, as evidenced by ESI-MS and CV. The DFT optimised structure of $[\text{Cu}(\text{4})(\text{5})]^{2+}$ suggests that ligand **5** is tilted toward the phenanthroline unit in a square pyramidal rather than trigonal bipyramidal geometry presumably due to the strong pyridyl→Cu binding (Cu \cdots N1 = 2.27 Å). The latter interaction draws the two mesityl groups of **5** toward each other and leaves little space for ligand **4**. Upon irreversible reduction of the freshly prepared $[\text{Cu}(\text{4})(\text{5})]^{2+}$ at $E_{pc} = 245$ mV a follow-up reaction occurs that is visible in the reverse anodic scan: the broad waves at $E_{pa} = 538$ & 720 mV may be assigned to the oxidation of a mixture of homo- and heteroleptic complexes (alike the complex mixture from **4**, **5** and Cu^+ , *vide supra*).



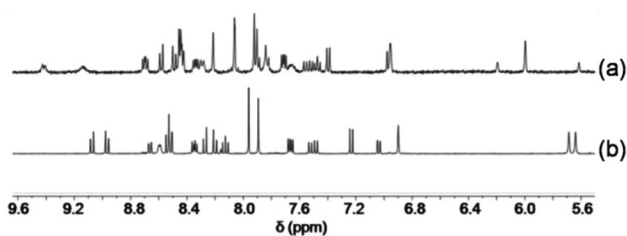


Fig. 3 Partial ^1H NMR spectra of equimolar mixtures (a) of **3**, **4**, **5** and Cu^+ (CD_2Cl_2) and (b) of **3**, **4**, **5** and Zn^{2+} (CD_2Cl_2 – CD_3CN = 3 : 1).

Self-sorting

To study self-sorting,¹⁷ a mixture of **3**, **4**, **5** and Cu^+ (1 : 1 : 1 : 1) was sonicated in CD_2Cl_2 . Although six copper(i) complexes may be expected, the ESI mass spectrum shows only two peaks at 800.3 Da and 1051.0 Da suggesting the exclusive formation of the complexes $[\text{Cu}(\mathbf{3})(\mathbf{4})]^+$ and $[\text{Cu}(\mathbf{5})_2]^+$, respectively (Fig. S36, ESI †). In full agreement, the ^1H NMR spectrum displays diagnostic peaks at 6.00 ppm for the heteroleptic complex $[\text{Cu}(\mathbf{3})(\mathbf{4})]^+$ and at 5.62 & 6.19 ppm for the homoleptic complex $[\text{Cu}(\mathbf{5})_2]^+$ (Fig. 3). Two sharp singlets at 5.64 and 5.69 ppm would have been diagnostic for $[\text{Cu}(\mathbf{4})(\mathbf{5})]^+$, but those signals are absent. NMR integration suggests that complexes $[\text{Cu}(\mathbf{3})(\mathbf{4})]^+$ and $[\text{Cu}(\mathbf{5})_2]^+$ are present in 89% : 11% along with unused ligands **3**, **4** and **5**.

When **3**, **4**, **5** and $\text{Zn}(\text{OTf})_2$ (1 : 1 : 1 : 1) were sonicated for 30 min in CD_2Cl_2 – CD_3CN (3 : 1), quantitative formation of the heteroleptic complex $[\text{Zn}(\mathbf{4})(\mathbf{5})]^{2+}$ was observed. The ^1H NMR spectrum shows singlets at 5.64 & 5.69 ppm that are diagnostic for the heteroleptic complex along with a CH_{Mes} signal at 6.94 ppm indicative for the ligand **3** (Fig. 3). The two peaks at 370.0 and 888.3 Da in the ESI mass spectrum correspond to the doubly charged $[\text{Zn}(\mathbf{4})(\mathbf{5})]^{2+}$ and singly charged $[\text{Zn}(\mathbf{4})(\mathbf{5})](\text{OTf})^+$, respectively (Fig. S38, ESI †). Due to the analogous d^{10} configuration of Zn^{2+} and Cu^{2+} , similar self-sorting phenomena are expected for both metal ions suggesting quantitative complex formation of $[\text{Cu}(\mathbf{4})(\mathbf{5})]^{2+}$ with **3** remaining untouched in solution.

The effect of changing the metal's oxidation state on self-sorting was studied by CV. In the anodic scan of an equimolar mixture of **3**, **4**, **5** and Cu^+ , the irreversible peak at $E_{\text{pa}} = 763$ mV is assigned to the oxidation of $[\text{Cu}(\mathbf{3})(\mathbf{4})]^+$. The oxidation wave of the homoleptic complex $[\text{Cu}(\mathbf{5})_2]^+$ ($E_{\text{pa}} = 720$ mV, *vide supra*) is hardly detectable due to its small amount (11%, see NMR). In the reverse scan, the irreversible reduction wave at $E_{\text{pc}} = 242$ mV indicates that the complex must have undergone a major reorganisation. Apparently, both $[\text{Cu}(\mathbf{3})(\mathbf{4})]^{2+}$ and $[\text{Cu}(\mathbf{5})_2]^{2+}$ undergo fast ligand shuffling in solution to afford exclusively the heteroleptic complex $[\text{Cu}(\mathbf{4})(\mathbf{5})]^{2+}$. After reduction of $[\text{Cu}(\mathbf{4})(\mathbf{5})]^{2+}$, the anodic back scan again shows the oxidation waves corresponding to complexes $[\text{Cu}(\mathbf{3})(\mathbf{4})]^+$ and $[\text{Cu}(\mathbf{5})_2]^+$ at $E_{\text{pa}} = 763$ mV. No oxidation wave was observed corresponding to $[\text{Cu}(\mathbf{4})(\mathbf{5})]^+$. In fact, both peaks did not show reversibility at any of chosen scan rates (from 50 to 200 mV s^{-1}) at this concentration ($c = 0.65$ mM). Randles–

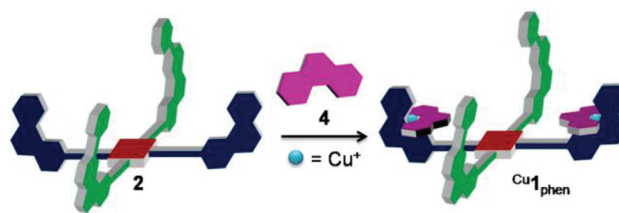


Fig. 4 Preparation of complex $\text{Cu}_1^{\text{phen}}$.

Sevcik plots yield a linear dependence of the anodic peak intensity i_{pa} with the square root of the scan rate ($\nu^{1/2}$), thus attesting a diffusion-limited electron-transfer process. This study clearly indicates fast metal ligand reorganisation upon changing the oxidation state of copper ($\text{Cu}^+ \rightarrow \text{Cu}^{2+} \rightarrow \text{Cu}^+$) or changing from copper(i) to zinc(ii) ions both resulting in a self-sorting between heteroleptic complexes.

Self-sorting on scaffold 2

To use the redox-triggered switching of the self-sorting process for cargo shipping between two different stations, the new ligand **2** is used as a nanoscaffold. At the outset, **2**, **4** and Cu^+ (1 : 2 : 2) were reacted in CD_2Cl_2 to afford the complex $\text{Cu}_1^{\text{phen}} = [\text{Cu}_2(\mathbf{2})(\mathbf{4})_2](\text{PF}_6)_2$, in which both PhenAr₂ stations of **2** are quantitatively occupied by $[\text{Cu}(\mathbf{4})]^+$, while the TerpyAr₂ stations remain unloaded (Fig. 4). The complex was characterised by ^1H NMR, ^1H – ^1H COSY and ESI-MS. ^1H NMR (Fig. 5) reveals that protons 9-H are upfield shifted from 6.94 to 6.00 ppm while protons 15'-H remain unchanged at 6.97 ppm (as in compound **2**). Other protons of the PhenAr₂ stations also undergo major shifts due to formation of the heteroleptic complex while protons of the TerpyAr₂ units remain unchanged (see Table S3 †). Formation of the complex is ascertained by a peak at 1565.1 Da in the ESI mass spectrum (Fig. S40, ESI †) corresponding to the doubly charged species $[\text{Cu}_2(\mathbf{2})(\mathbf{4})_2]^{2+}$ after loss of two counteranions (PF_6^-). Finally, the ^1H DOSY trace proves that assembly $\text{Cu}_1^{\text{phen}}$ exists in solution as a single species (Fig. S50, ESI †).

When a 1 : 2 mixture of **2** and **4** was treated with 2 equiv. of $\text{Cu}(\text{ClO}_4)_2 \cdot 6\text{H}_2\text{O}$, complex $\text{Cu}_1^{\text{terpy}} = [\text{Cu}_2(\mathbf{2})(\mathbf{4})_2](\text{ClO}_4)_4$ formed quantitatively as derived from the ESI-MS data. They (Fig. S42, ESI †) show two peaks at 782.7 Da and 1076.8 Da corresponding to the quadruply-charged $[\text{Cu}_2(\mathbf{2})(\mathbf{4})_2]^{4+}$ and triply-charged species $[\text{Cu}_2(\mathbf{2})(\mathbf{4})_2](\text{ClO}_4)^{3+}$ after loss of four and three-counter anions (ClO_4^-), respectively. Strong paramagnetic broadening by Cu^{2+} prevented us from characterising the complex by ^1H NMR. However, expecting a similar coordination behaviour of zinc(ii) and copper(ii) ions (*vide supra* for the model study), we reacted Zn^{2+} with **1** and **4** (2 : 1 : 2). As a result, complex $\text{Zn}_1^{\text{terpy}}$ was afforded, in which the $[\text{Zn}(\mathbf{4})]^{2+}$ units quantitatively occupy the TerpyAr₂ stations with the PhenAr₂ stations remaining unloaded. Diagnostically, the ^1H NMR (see Fig. 5, Table S4 †) showed protons 15'-H (TerpyAr₂) to be shifted upfield to 5.69 ppm while protons 9-H of both PhenAr₂ units remain unaltered at 6.91 ppm. A similar behaviour was observed for other protons of the PhenAr₂ and TerpyAr₂ units. In the ESI mass spectrum (Fig. S41, ESI †), $\text{Zn}_1^{\text{terpy}}$ exhibited



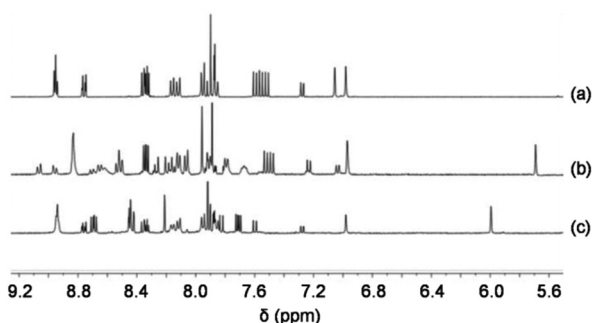


Fig. 5 Partial ^1H NMR spectra of (a) **2** (CD_2Cl_2), (b) $\text{Zn}^{\text{I}}_{\text{terpy}}$ (CD_2Cl_2 - $\text{CD}_3\text{CN} = 3:1$) and (c) $\text{Cu}^{\text{I}}_{\text{phen}}$ (CD_2Cl_2).

three peaks at 783.5 Da, 1094.4 Da and 1716.1 Da that are assigned to quadruply-charged ($[\text{Zn}_2(\text{2})(\text{4})_2]^{4+}$), triply-charged ($[\text{Zn}_2(\text{2})(\text{4})_2](\text{OTf})^{3+}$) and doubly-charged ($[\text{Zn}_2(\text{2})(\text{4})_2](\text{OTf})_2^{2+}$) species after loss of four, three and two counter anions (OTf^-), respectively. Finally, ^1H DOSY suggests that $\text{Zn}^{\text{I}}_{\text{terpy}}$ exists in solution as a single species (Fig. S51, ESI †).

Electrochemical cargo shipping

Inspired by the reversible interconversion of two heteroleptic complexes *via* electrochemical means, both complexes $\text{Cu}^{\text{I}}_{\text{phen}}$ and $\text{Cu}^{\text{I}}_{\text{terpy}}$ were tested for cargo shipping between the two different stations (PhenAr $_2$ and TerpyAr $_2$) on scaffold **2**. In the CV, complex $\text{Cu}^{\text{I}}_{\text{terpy}} = [\text{Cu}_2(\text{2})(\text{4})_2](\text{ClO}_4)_4$ (scan rate = 100 mV s^{-1}) exhibits an irreversible reduction wave at $E_{\text{pc}} = 246 \text{ mV}$ (Fig. 6, right) that is characteristic for a pentacoordinated copper(II) complex (inverse HETTAP complex). On the reverse scan, the oxidation of the reduced species displays an irreversible peak at $E_{\text{pa}} = 786 \text{ mV}$ that is characteristic for oxidation of a copper(I/II) HETPHEN complex (unfortunately, the peak is merged with the first reversible oxidation peak of the zinc(II) porphyrin unit with $E_{\text{pa}} = 830 \text{ mV}$ and $E_{1/2} = 790 \text{ mV}$). Shifting the cathodic switching potential towards negative potential (by $\Delta E_1 = -100 \text{ mV}$) and thus increasing the time for rearrangement increases the anodic current (i_{pa}) at $E_{\text{pa}} = 786 \text{ mV}$ (see ESI †) clearly arguing for ligand translocation from the TerpyAr $_2$ to PhenAr $_2$ stations upon reduction of Cu^{2+} to Cu^+ . Anodic peak current (i_{pa}) enhancement at $E_{\text{pa}} = 786 \text{ mV}$ is also observed when using a 5 s delay at the first switching potential ($E_1 = -100 \text{ mV}$). Moreover, both peaks show hardly any reversible behaviour in the scan rate range (50 to 1000 mV s^{-1}).

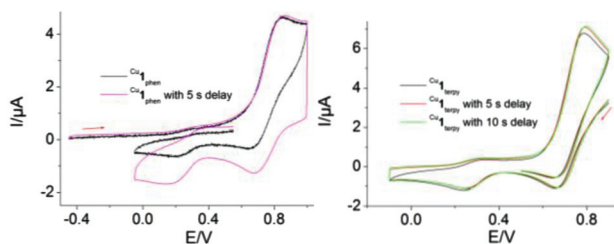


Fig. 6 Cyclic voltammogram of (left) $\text{Cu}^{\text{I}}_{\text{phen}}$ (scan rate = 500 mV s^{-1}) and (right) $\text{Cu}^{\text{I}}_{\text{terpy}}$ (scan rate = 100 mV s^{-1}) in dry CH_2Cl_2 .

Similarly, when HETPHEN complex $\text{Cu}^{\text{I}}_{\text{phen}} = [\text{Cu}_2(\text{2})(\text{4})_2](\text{PF}_6)_2$ is electrochemically oxidised at $\nu = 500 \text{ mV s}^{-1}$, the oxidation wave is irreversible ($E_{\text{pa}} = 844 \text{ mV}$). The wave overlaps with the first oxidation potential of the zinc(II) porphyrin (por/por $^{2+}$; Fig. 6, left). In the reverse reductive scan, an irreversible peak is observed at $E_{\text{pc}} = 174 \text{ mV}$ that is assigned to the reduction of electrochemically produced $\text{Cu}^{\text{I}}_{\text{terpy}}$ indicating metal and ligand translocation from PhenAr $_2$ to TerpyAr $_2$ stations. A time delay of 5 s at the first switching potential ($E_1 = 900 \text{ mV}$) increases the current of the $\text{Cu}^{2+}/\text{Cu}^+$ redox couple ($E_{1/2} = 269 \text{ mV}$) at the TerpyAr $_2$ station. Hence, CV studies clearly establish the reversible interconversion between the two stable species $\text{Cu}^{\text{I}}_{\text{phen}}$ and $\text{Cu}^{\text{I}}_{\text{terpy}}$ through cargo transport (Fig. 1).

The CV behaviour can be understood as an EC process. Electron transfer is followed by fast translocation of both metal ion and ligand between the two different stations. Simulation of the mechanism by DigiSim $^\circ$ was possible using a simplified scheme. Due to the fact that the rate constants for both cargo transport processes are hidden in each individual CV trace, one is able to even cross-check the data. Accordingly, the best agreement for $\text{Cu}^{2+}_{\text{PhenAr}_2} \rightarrow \text{Cu}^{2+}_{\text{TerpyAr}_2}$ was $K = 10$ and $k = 10 \text{ s}^{-1}$ and for $\text{Cu}^+_{\text{TerpyAr}_2} \rightarrow \text{Cu}^+_{\text{PhenAr}_2}$ was $K = 20$ and $k = 5 \text{ s}^{-1}$ (Fig. S49, ESI †). Using the same rate constants, also the redox-mediated shuttling between $[\text{Cu}(\text{3})(\text{4})]^+ + 5$ and $[\text{Cu}(\text{4})(\text{5})]^{2+} + 3$ (Fig. S44 †) was successfully simulated, lending further credibility to the above values. Moreover, a concentration-dependent CV study of $\text{Cu}^{\text{I}}_{\text{phen}}$ indicated negligible effects on the reversibility at $E_{1/2} = 263 \text{ mV}$ (Fig. S48, ESI †), suggesting that dissociation is rate-limiting. A plausible mechanism for shipping is thus the rate-determining release of the labilised metal ions (after oxidation/reduction) on the sub-second time scale along with their phenanthroline cargo from a particular station followed by fast reassociation at the other station (a bimolecular process), which can be either intra- or intersupramolecular.

Conclusion

In conclusion, we have shown that two heteroleptic complexes can be interconverted by changing the oxidation state of the copper ions. Using this redox-triggered self-sorting, cargo (ligand **4** and copper) may be shipped reversibly between two different stations (PhenAr $_2$ and TerpyAr $_2$) on platform **2**. If the redox state at copper is +I, ligand **4** occupies quantitatively the PhenAr $_2$ stations, whereas for copper(II), the TerpyAr $_2$ stations are engaged with the cargo molecules. Electrochemical oxidation and reduction leads to reversible shipping of the cargo between the two different stations. Concentration-dependent CV studies advocate that dissociation of the cargo from the scaffold is the rate determining step.

Experimental procedure

Commercial reagents were used without further purification. Solvents were dried with appropriate desiccants and distilled



prior to use. ^1H and ^{13}C NMR spectra were recorded at 400 MHz or 600 MHz using a deuterated solvent as the lock and residual protiated solvent as internal reference. The following abbreviations are utilised to describe NMR peak patterns: s = singlet, d = doublet, t = triplet, dd = doublet of doublets. The following abbreviations are used to describe peak patterns of IR spectra: s = sharp, m = medium, w = weak. The numbering of the carbon skeleton in molecular formulae as shown in the manuscript does not comply with the IUPAC nomenclature rules; it is only used for assignments of NMR signals. Electrospray ionisation (ESI) mass spectra were recorded on a Thermo-Quest LCQ deca. Melting points were measured on a Büchi SMP-20 and are uncorrected. Infrared spectra were recorded on a Varian 1000 FT-IR instrument. Elemental analysis measurements were made using the EA 3000 CHNS. Cyclic voltammetry (CV) was measured on a Parstat 2273. CV of millimolar solutions was carried out in dry CH_2Cl_2 (2.0 mL) with 0.1 M *n*-Bu₄NPF₆ as electrolyte against a Ag wire as a quasi-reference electrode and triphenylpyrylium tetrafluoroborate (TPP) as internal standard. All CV spectra are calibrated against the standard calomel electrode (SCE).

2-(2,4,6-Trimethylphenyl)-6-bromopyridine (6)

2,6-Dibromopyridine (2.16 g, 9.12 mmol), 2,4,6-trimethylphenylboronic acid (1.60 g, 6.10 mmol) and Pd(PPh₃)₄ (70.0 mg, 60.6 μmol) were dissolved in a degassed solution of MeOH (40 mL), THF (100 mL) and aqueous K₂CO₃ (2 M, 30 mL), then the solution was refluxed for 12 h at 90 °C. The solvent was evaporated and the residue redissolved in DCM. The organic phase was washed with water thrice and then dried over anhydrous Na₂SO₄. The product was further purified by column chromatography (SiO₂, hexane–EtOAc = 9 : 1, *R*_f = 0.3) to afford a liquid. Yield: 90%, ^1H NMR (CDCl₃, 400 MHz): δ = 2.04 (s, 6 H, CH₃), 2.31 (s, 3 H, CH₃), 6.92 (s, 2 H, 15'-H), 7.18 (dd, $^3J = 7.8$ Hz, $^4J = 0.8$ Hz, 1 H, 14-H), 7.45 (dd, $^3J = 7.8$ Hz, $^4J = 0.8$ Hz, 1 H, 12-H), 7.61 (t, $^3J = 7.8$ Hz, 1 H, 13-H) ppm. ^{13}C NMR (CDCl₃, 100 MHz): δ = 20.1, 21.0, 123.7, 125.9, 128.3, 135.6, 136.2, 137.9, 138.5, 141.7, 161.1 ppm. IR (KBr): $\tilde{\nu} = 3944, 3690, 3055, 2986, 2306, 1571, 1425, 1265, 741$ cm⁻¹. ESI-MS: *m/z* (%) 277.1 (100) [M + H]⁺. Anal Calcd for C₁₄H₁₄BrN·0.2H₂O: C, 60.10; H, 5.19; N, 5.01. Found: C, 60.06; H, 5.17; N, 5.20.

2-(6-(2,4,6-Trimethylphenyl)pyrid-2-yl)-9-(2,4,6-trimethylphenyl)-[1,10]-phenanthroline (5)

To a solution of **6** (841 mg, 3.05 mmol) in dry diethyl ether (80 mL), 2.5 M *n*-BuLi (1.22 mL, 3.05 mmol) in hexane was added dropwise at -78 °C under N₂ atmosphere over a period of 15 min. The reaction mixture was stirred at -40 °C for 2 h, then 2-(2,4,6-trimethylphenyl)-[1,10]-phenanthroline (605 mg, 2.03 mmol) was added under N₂ atmosphere. The solution turned immediately dark violet. After stirring for another 12 h at room temperature, saturated aqueous NH₄Cl (100 mL) was added. The reaction slurry was stirred for 1 h, then the solution was extracted with DCM (3 × 100 mL). After drying over anhydrous Na₂SO₄, the solvent was removed. The solid orange residue was dissolved in DCM (100 mL) and treated with MnO₂

(2.65 g, 30.5 mmol). After stirring for 12 h at room temperature, the solution was filtered through a pad of celite. The solvent was evaporated to dryness. Finally, the compound was purified by column chromatography (SiO₂, hexane–ethyl acetate = 9 : 1, *R*_f = 0.4). Yield: 54%, mp: 236 °C. ^1H NMR (CD₂Cl₂, 400 MHz): δ = 2.10 (s, 6 H, CH₃), 2.26 (s, 6 H, CH₃), 2.35 (s, 3 H, CH₃), 2.40 (s, 3 H, CH₃), 6.98 (s, 2 H, [15 or 15']-H), 7.04 (s, 2 H, [15' or 15]-H), 7.25 (dd, $^3J = 7.4$ Hz, $^4J = 1.0$ Hz, 1 H, 14-H), 7.62 (d, $^3J = 8.4$ Hz, 1 H, 4'-H), 7.84 (s, 2 H, 5', 6'-H), 7.92 (t, $^3J = 7.4$ Hz, 1 H, 13-H), 8.29 (d, $^3J = 8.4$ Hz, 1 H, 3'-H), 8.31 (d, $^3J = 8.4$ Hz, 1 H, 8'-H), 8.78 (d, $^3J = 8.4$ Hz, 1 H, 7'-H), 8.81 (dd, $^3J = 7.4$ Hz, $^4J = 1.0$ Hz, 1 H, 12-H) ppm. ^{13}C NMR (CD₂Cl₂, 100 MHz): δ = 19.6, 20.7, 20.9, 21.7, 118.4, 118.8, 118.9, 127.6, 130.5, 130.8, 130.9, 131.1, 131.2, 131.7, 132.4, 132.7, 134.8, 135.6, 136.0, 136.5, 137.4, 138.9, 139.2, 142.5, 149.4, 149.7, 149.9, 160.2, 160.8 ppm. IR (KBr): $\tilde{\nu} = 3001, 2943, 2913, 1583, 1541, 1477, 1374, 1355, 1158, 1134, 909, 862, 847, 752, 637, 629$ cm⁻¹. ESI-MS: *m/z* (%) 494.4 (100) [M + H]⁺. Anal Calcd for C₃₅H₃₁N₃·0.2H₂O: C, 84.54; H, 6.36; N, 8.45. Found: C, 84.46; H, 6.15; N, 8.82.

2-(6-(2,4,6-Trimethylphenyl)pyrid-2-yl)-[1,10]-phenanthroline (7)

Under N₂ atmosphere, 2.5 M *n*-BuLi (1.45 mL, 3.62 mmol) in hexane was added dropwise to a solution of **6** (1.00 g, 3.62 mmol) in dry diethyl ether (80 mL) at -78 °C over a period of 15 min. The reaction mixture was stirred at -40 °C for 2 h, then [1,10]-phenanthroline (489 mg, 2.72 mmol) was added under N₂ atmosphere. The solution turning immediately to a dark violet was stirred for another 12 h at room temperature. Saturated aqueous NH₄Cl (100 mL) was then added and the reaction slurry was stirred for 1 h. Thereafter, the solution was extracted with DCM (3 × 100 mL). After drying over anhydrous Na₂SO₄, the solvent was removed. The solid orange residue was dissolved in DCM (100 mL) and treated with MnO₂ (3.15 g, 36.2 mmol). After stirring for 12 h at room temperature, the solution was filtered through a pad of celite. The solvent was evaporated to dryness. Finally, the compound was purified by column chromatography (SiO₂, DCM–ethyl acetate = 1 : 3, *R*_f = 0.25). Yield: 61%, mp: 165 °C. ^1H NMR (CD₂Cl₂, 400 MHz): δ = 2.01 (s, 6 H, CH₃), 2.34 (s, 3 H, CH₃), 6.91 (s, 2 H, 15-H), 7.23 (dd, $^3J = 7.6$ Hz, $^4J = 1.2$ Hz, 1 H, 14-H), 7.55 (d, $^3J = 8.0$ Hz, 1 H, 8'-H), 7.63 (dd, $^3J = 8.0$ Hz, $^3J = 4.4$ Hz, 1 H, 3'-H), 7.82 (d, $^3J = 8.8$ Hz, 1 H, [5' or 6']-H), 7.86 (d, $^3J = 8.8$ Hz, 1 H, [6' or 5']-H), 7.94 (t, $^3J = 7.6$ Hz, 1 H, 13-H), 8.28 (d, $^3J = 8.0$ Hz, 2 H, 4', 7'-H), 8.83 (dd, $^3J = 7.6$ Hz, $^4J = 1.2$ Hz, 1 H, 12-H), 9.21 (dd, $^3J = 4.4$ Hz, $^3J = 1.6$ Hz, 1 H, 2'-H) ppm. ^{13}C NMR (CD₂Cl₂, 100 MHz): δ = 19.6, 20.7, 124.8, 125.0, 127.6, 128.5, 130.5, 130.8, 130.9, 131.7, 132.6, 135.6, 135.9, 136.0, 136.0, 137.4, 137.6, 138.0, 141.4, 146.1, 146.1, 160.3, 160.9 ppm. IR (KBr): $\tilde{\nu} = 2967, 2923, 1583, 1521, 1447, 1374, 1365, 1158, 1134, 919, 856$ cm⁻¹. ESI-MS: *m/z* (%) 376.4 (100) [M + H]⁺. Anal Calcd for C₂₆H₂₁N₃·CH₂Cl₂: C, 70.44; H, 5.04; N, 9.13. Found: C, 70.67; H, 5.15; N, 8.82.



2-(6-(2,4,6-Trimethylphenyl)pyrid-2-yl)-9-(4-iodo-2,3,5,6-tetramethylphenyl)-[1,10]-phenanthroline (**8**)

Over a period of 15 min, 2.5 M *n*-BuLi (0.800 mL, 2.00 mmol) in hexane was added dropwise at $-78\text{ }^{\circ}\text{C}$ under N_2 atmosphere to a solution of 1,4-diiodo-2,3,5,6-tetramethylbenzene (770 mg, 2.00 mmol) in dry diethyl ether (80 mL). The reaction mixture was stirred at $-40\text{ }^{\circ}\text{C}$ for 2 h, then **7** (500 mg, 1.33 mmol) was added under N_2 atmosphere. The solution turning immediately to dark violet was stirred for another 12 h at room temperature. Saturated aqueous NH_4Cl (100 mL) was then added and the reaction slurry was stirred for 1 h. Thereafter, the solution was extracted with DCM ($3 \times 100\text{ mL}$). After drying over anhydrous Na_2SO_4 , the solvent was removed. The solid orange residue, redissolved in DCM (100 mL), was treated with MnO_2 (1.72 g, 20.0 mmol) for 12 h at room temperature. After passing the solution through a pad of celite, the solvent was removed. Finally, the compound was purified by column chromatography (SiO_2 , DCM-ethyl acetate = 70:30, $R_f = 0.4$). Yield: 53%, mp: $>213\text{ }^{\circ}\text{C}$. $^1\text{H NMR}$ (CD_2Cl_2 , 400 MHz): $\delta = 2.09$ (s, 6 H, CH_3), 2.24 (s, 6 H, CH_3), 2.33 (s, 6 H, CH_3), 2.40 (s, 3 H, CH_3), 6.97 (s, 2 H, 15'-H), 7.28 (dd, $^3J = 7.6\text{ Hz}$, $^4J = 0.8\text{ Hz}$, 1 H, 14-H), 7.60 (d, $^3J = 8.4\text{ Hz}$, 1 H, 4'-H), 7.87 (s, 2 H, 5', 6'-H), 7.94 (t, $^3J = 7.6\text{ Hz}$, 1 H, 13-H), 8.34 (d, $^3J = 8.4\text{ Hz}$, 1 H, 3'-H), 8.35 (d, $^3J = 8.4\text{ Hz}$, 1 H, 8'-H), 8.75 (d, $^3J = 8.4\text{ Hz}$, 1 H, 7'-H), 8.77 (dd, $^3J = 7.6\text{ Hz}$, $^4J = 0.8\text{ Hz}$, 1 H, 12-H) ppm. $^{13}\text{C NMR}$ (CD_2Cl_2 , 100 MHz): $\delta = 19.3$, 20.7, 21.6, 21.9, 118.6, 124.6, 124.9, 127.6, 129.7, 130.5, 130.8, 130.9, 132.4, 132.9, 134.5, 135.1, 135.9, 136.2, 136.9, 137.4, 137.6, 138.5, 141.3, 142.3, 143.5, 146.1, 146.1, 160.3, 160.9 ppm. IR (KBr): $\tilde{\nu} = 2956$, 2916, 1565, 1521, 1454, 1354, 1324, 1158, 1126, 919, 887 cm^{-1} . ESI-MS: m/z (%) 637.4 (100) $[\text{M} + \text{H}]^+$. Anal Calcd for $\text{C}_{36}\text{H}_{32}\text{I}_2\text{N}_3 \cdot \text{CH}_3\text{CO}_2\text{C}_2\text{H}_5$: C, 62.62; H, 6.76; N, 3.91. Found: C, 62.46; H, 6.45; N, 3.82.

Zinc(II) porphyrin **10**

Zinc(II)-5,15-bis(4-iodophenyl)-10,20-bis(4-trimethylsilylethynylphenyl)porphyrin (250 mg, 223 μmol) and phenanthroline **9** (203 mg, 446 μmol) were placed in a round-bottomed flask. Then, $\text{Pd}(\text{PPh}_3)_4$ (25.7 mg, 22.3 μmol), dry NEt_3 (10 mL) and dry DMF (30 mL) were added under N_2 atmosphere. The reaction mixture was allowed to stir at $90\text{ }^{\circ}\text{C}$ for 12 h. Then, it was evaporated to dryness, dissolved in DCM (50 mL), and washed with water ($3 \times 50\text{ mL}$). After drying over anhydrous Na_2SO_4 , the solvent was evaporated and the residue was purified by column chromatography (SiO_2 , hexane-EtOAc = 80:20, $R_f = 0.4$). The compound was further purified by size exclusion chromatography over biobeads SX-3 isolating the first moving band in toluene. Yield: 58%, mp: $>300\text{ }^{\circ}\text{C}$. $^1\text{H NMR}$ (400 MHz, CD_2Cl_2): $\delta = 0.38$ (s, 18 H, TMS-H), 2.04 (s, 12 H, CH_3), 2.12 (s, 12 H, CH_3), 2.31 (s, 6 H, CH_3), 2.54 (s, 12 H, CH_3), 6.92 (s, 4 H, 9-H), 7.52 (d, $^3J = 8.4\text{ Hz}$, 2 H, 7-H), 7.59 (d, $^3J = 8.4\text{ Hz}$, 2 H, 4-H), 7.87 (d, $^3J = 8.4\text{ Hz}$, 4 H, 11-H), 7.88 (s, 4 H, 5-, 6-H), 7.93 (d, $^3J = 8.4\text{ Hz}$, 4 H, 17-H), 8.10 (d, $^3J = 8.4\text{ Hz}$, 4 H, 10-H), 8.15 (d, $^3J = 8.4\text{ Hz}$, 4 H, 16-H), 8.36 (d, $^3J = 8.4\text{ Hz}$, 2 H, 8-H), 8.54 (d, $^3J = 8.4\text{ Hz}$, 2 H, 3-H), 8.92 (d, $^3J = 4.0\text{ Hz}$, 4 H, β -H), 8.94 (d,

$^3J = 4.8\text{ Hz}$, 4 H, β -H) ppm. $^{13}\text{C NMR}$ (100 MHz, CD_2Cl_2): $\delta = 0.1$, 19.6, 20.5, 21.0, 27.6, 93.9, 94.0, 95.4, 95.5, 105.0, 111.8, 119.9, 120.6, 122.4, 124.8, 125.0, 126.1, 126.4, 127.2, 127.2, 128.4 (2C), 130.2, 131.9, 132.0, 132.0, 132.6, 134.2, 135.7, 135.8, 136.0, 136.0, 137.5, 137.6, 141.4, 142.1, 142.8, 146.0, 149.8, 149.9, 149.9, 160.2, 160.8 ppm. IR (KBr): $\tilde{\nu} = 2947$, 2928, 2815, 2320, 2343, 1609, 1556, 1490, 1416, 1380, 1356, 1185, 1099, 1025, 998, 884 cm^{-1} . ESI-MS: m/z (%) 1774.5 (100) $[\text{M} + \text{H}]^+$. Anal Calcd for $\text{C}_{120}\text{H}_{100}\text{N}_8\text{Si}_2\text{Zn} \cdot 2\text{H}_2\text{O}$: C, 79.55; H, 5.79; N, 6.18. Found: C, 79.92; H, 6.19; N, 6.22.

Zinc(II) porphyrin **11**

KOH (96.0 mg, 1.71 mmol) was added to a solution of zinc(II) porphyrin **10** (310 mg, 0.175 mmol) in THF (30 mL). Then, MeOH (15 mL) and H_2O (5 mL) were added, and the reaction mixture was stirred for 12 h at room temperature. After evaporating the solvent, the residue was redissolved in DCM and washed with water ($3 \times 100\text{ mL}$). After drying over anhydrous Na_2SO_4 , DCM was evaporated and the compound was used without further purification. Yield: 90%, mp: $>300\text{ }^{\circ}\text{C}$. $^1\text{H NMR}$ (400 MHz, CD_2Cl_2): $\delta = 2.04$ (s, 12 H, CH_3), 2.14 (s, 12 H, CH_3), 2.33 (s, 6 H, CH_3), 2.53 (s, 12 H, CH_3), 3.61 (s, 2 H, ethynyl-H), 6.92 (s, 4 H, 9-H), 7.54 (d, $^3J = 8.4\text{ Hz}$, 2 H, 7-H), 7.58 (d, $^3J = 8.4\text{ Hz}$, 2 H, 4-H), 7.86 (d, $^3J = 8.4\text{ Hz}$, 4 H, 11-H), 7.90 (s, 4 H, 5-, 6-H), 7.98 (d, $^3J = 8.4\text{ Hz}$, 4 H, 17-H), 8.11 (d, $^3J = 8.4\text{ Hz}$, 4 H, 10-H), 8.19 (d, $^3J = 8.4\text{ Hz}$, 4 H, 16-H), 8.37 (d, $^3J = 8.4\text{ Hz}$, 2 H, 8-H), 8.56 (d, $^3J = 8.4\text{ Hz}$, 2 H, 3-H), 8.90 (d, $^3J = 4.0\text{ Hz}$, 4 H, β -H), 8.95 (d, $^3J = 4.8\text{ Hz}$, 4 H, β -H) ppm. $^{13}\text{C NMR}$ (100 MHz, CD_2Cl_2): $\delta = 19.4$, 20.7, 21.6, 27.4, 93.1, 94.0, 95.1, 95.6, 105.3, 111.1, 119.9, 120.6, 122.4, 124.8, 125.2, 126.7, 126.8, 127.2, 127.3, 128.6, 128.7, 130.5, 131.8, 132.1, 132.3, 132.6, 134.6, 135.8, 135.9, 136.2, 136.3, 137.6, 137.8, 141.4, 142.5, 142.8, 146.1, 149.8, 149.9, 150.1, 160.2, 160.8 ppm. IR (KBr): $\tilde{\nu} = 2998$, 2935, 2820, 2345, 2323, 1619, 1565, 1490, 1397, 1353, 1189, 1050, 1025, 945, 895 cm^{-1} . ESI-MS: m/z (%) 1630.3 (100) $[\text{M} + \text{H}]^+$. Anal Calcd for $\text{C}_{116}\text{H}_{96}\text{N}_8\text{Zn}_2$: C, 80.48; H, 5.05; N, 6.53. Found: C, 80.67; H, 5.29; N, 6.32.

Zinc(II) porphyrin **2**

Zinc(II) porphyrin **11** (110 mg, 67.4 μmol) and phenanthroline **8** (85.5 mg, 135 μmol) were put into a round-bottomed flask. Then, $\text{Pd}(\text{PPh}_3)_4$ (15.6 mg, 13.5 μmol), dry NEt_3 (10 mL) and dry DMF (30 mL) were added to the reaction mixture under N_2 atmosphere. The reaction mixture was allowed to stir at $90\text{ }^{\circ}\text{C}$ for 12 h. The reaction mixture was evaporated to dryness, dissolved in DCM (50 mL), and washed with water ($3 \times 50\text{ mL}$). After drying over anhydrous Na_2SO_4 , the solvent was evaporated and the residue was purified by column chromatography (SiO_2 , DCM-MeOH = 99:1, $R_f = 0.1$). The compound was further purified by size exclusion chromatography over biobeads SX-3 isolating the first moving band in toluene. Yield: 35%, mp: $>300\text{ }^{\circ}\text{C}$. $^1\text{H NMR}$ (400 MHz, CD_2Cl_2): $\delta = 2.00$ (s, 12 H, CH_3), 2.03 (s, 12 H, CH_3), 2.09 (s, 12 H, CH_3), 2.16 (s, 12 H, CH_3), 2.33 (s, 6 H, CH_3), 2.35 (s, 6 H, CH_3), 2.41 (s, 12 H, CH_3), 2.60 (s, 12 H, CH_3), 6.95 (s, 4 H, 9-H), 6.98 (s, 4 H, 15'-H), 7.28 (dd, $^3J = 7.6\text{ Hz}$, $^4J = 0.8\text{ Hz}$, 2 H, 14-H), 7.52 (d, $^3J = 8.0\text{ Hz}$,



2 H, [4 or 7]-H), 7.56 (d, $^3J = 8.0$ Hz, 2 H, [7 or 4]-H), 7.60 (d, $^3J = 8.4$ Hz, 2 H, 4'-H), 7.86 (d, $^3J = 8.4$ Hz, 4 H, [17 or 16]-H), 7.87 (s, 4 H, 5', 6'-H), 7.90 (s, 4 H, 5-, 6-H), 7.95 (d, $^3J = 8.4$ Hz, 4 H, [11 or 10]-H), 7.94 (t, $^3J = 7.6$ Hz, 2 H, 13-H), 8.12 (d, $^3J = 8.4$ Hz, 4 H, [10 or 11]-H), 8.16 (d, $^3J = 8.4$ Hz, 4 H, [16 or 17]-H), 8.33 (d, $^3J = 8.0$ Hz, 2 H, [3 or 8]-H), 8.34 (d, $^3J = 8.0$ Hz, 2 H, [8 or 3]-H), 8.34 (d, $^3J = 8.4$ Hz, 2 H, 3'-H), 8.36 (d, $^3J = 8.4$ Hz, 2 H, 8'-H), 8.76 (d, $^3J = 8.4$ Hz, 2 H, 7'-H), 8.77 (dd, $^3J = 7.6$ Hz, $^4J = 0.8$ Hz, 2 H, 12-H), 8.95 (d, $^3J = 4.4$ Hz, 4 H, β -H), 8.96 (d, $^3J = 4.4$ Hz, 4 H, β -H) ppm. ^{13}C NMR (100 MHz, CD_2Cl_2): $\delta = 20.0, 20.1, 20.6, 20.8, 21.5, 21.6, 28.0, 28.1, 94.4, 94.6, 97.2, 97.4, 112.5, 112.7, 120.2, 120.3, 120.9, 121.0, 122.7, 123.4, 124.0, 124.4, 124.9, 125.2, 126.3, 126.6, 126.9$ (2C), 127.0, 127.5, 127.6, 127.6, 128.8 (2C), 129.1, 129.2, 130.7, 132.4, 133.1 (2C), 134.7, 136.1, 136.2, 136.4, 136.4, 136.5, 136.6, 136.8, 138.0, 138.3, 138.4, 138.6, 138.6, 139.1 (2C), 141.5, 141.9, 141.9, 142.3, 142.3, 143.0, 146.4, 146.4, 146.6, 150.1, 150.1, 150.2, 150.6, 160.3, 160.9, 160.9 ppm. IR (KBr): $\tilde{\nu} = 2936, 2916, 2836, 2380, 2343, 1619, 1556, 1490, 1425, 1356, 1326, 1165, 1099$ cm^{-1} . ESI-MS: m/z (%) 1322.3 (100) $[\text{M} + 2\text{H}]^{2+}$, 881.9 (50) $[\text{M} + 3\text{H}]^{3+}$, 661.7 (30) $[\text{M} + 4\text{H}]^{4+}$. Anal. Calcd for $\text{C}_{186}\text{H}_{146}\text{N}_{14}\text{Zn} \cdot 1.5\text{CH}_2\text{Cl}_2$: C, 81.30; H, 5.42; N, 7.08. Found: C, 81.45; H, 5.19; N, 7.22.

Homoleptic complex $[\text{Cu}(5)_2](\text{PF}_6)$

In an NMR tube, ligand 5 (0.373 mg, 0.756 μmol) and $[\text{Cu}(\text{CH}_3\text{CN})_4]\text{PF}_6$ (0.141 mg, 0.378 μmol) were dissolved in CD_2Cl_2 to afford the desired complex in quantitative yield. mp: >300 $^\circ\text{C}$. ^1H NMR (CD_2Cl_2 , 400 MHz): $\delta = 0.70$ (s, 6 H, CH_3), 0.79 (s, 6 H, CH_3), 1.97 (s, 12 H, CH_3), 2.00 (s, 6 H, CH_3), 2.24 (s, 6 H, CH_3), 5.61 (s, 4 H, [15 or 15']-H), 6.19 (s, 4 H, [15' or 15]-H), 6.97 (dd, $^3J = 7.6$ Hz, $^3J = 1.2$ Hz, 2 H, 14-H), 7.40 (d, $^3J = 8.0$ Hz, 2 H, 4'-H), 7.47 (t, $^3J = 7.6$ Hz, 2 H, 13-H), 8.06 (s, 4 H, 5', 6'-H), 8.44 (d, $^3J = 8.0$ Hz, 2 H, 3'-H), 8.49 (d, $^3J = 8.6$ Hz, 2 H, 8'-H), 8.58 (d, $^3J = 8.6$ Hz, 2 H, 7'-H), 9.41 (dd, $^3J = 7.6$ Hz, $^3J = 1.2$ Hz, 2 H, 12-H) ppm. ^{13}C NMR (CD_2Cl_2 , 100 MHz): $\delta = 19.6, 19.8, 20.3, 21.0, 21.0, 122.5, 124.7, 126.1, 126.6, 126.9, 127.1, 127.2, 128.3, 128.4, 128.6, 130.1, 133.5, 135.6, 135.8, 136.0, 137.2, 137.3, 137.6, 137.6, 137.8, 144.1, 145.1, 153.5, 154.5, 159.7, 160.0$ ppm. IR (KBr): $\tilde{\nu} = 2965, 2903, 1613, 1585, 1454, 1402, 1339, 1138, 1104, 845, 810, 759$ cm^{-1} . ESI-MS: m/z (%) 1051.0 (100) $[\text{Cu}(5)_2]^+$. Anal. Calcd for $\text{C}_{70}\text{H}_{62}\text{CuF}_6\text{N}_6\text{P}$: C, 70.31; H, 5.23; N, 7.03. Found: C, 70.36; H, 5.45; N, 7.15.

Heteroleptic complex $[\text{Zn}(4)(5)](\text{OTf})_2$

In an NMR tube, compound 5 (0.550 mg, 1.11 μmol), $\text{Zn}(\text{OTf})_2$ (0.405 mg, 1.11 μmol) and 4 (0.201 mg, 1.11 μmol) were dissolved in CD_2Cl_2 - $\text{CD}_3\text{CN} = 3:1$ furnishing the desired complex in quantitative yield. mp: >300 $^\circ\text{C}$. ^1H NMR (CD_2Cl_2 - $\text{CD}_3\text{CN} = 3:1$, 400 MHz): $\delta = 0.93$ (s, 6 H, CH_3), 1.00 (s, 6 H, CH_3), 1.82 (s, 3 H, CH_3), 1.87 (s, 3 H, CH_3), 5.64 (s, 2 H, [15 or 15']-H), 5.69 (s, 2 H, [15' or 15]-H), 7.04 (dd, $^3J = 7.6$ Hz, $^4J = 1.2$ Hz, 1 H, 14-H), 7.23 (d, $^3J = 8.4$ Hz, 1 H, 4'-H), 7.67 (dd, $^3J = 8.4$ Hz, $^3J = 8.4$ Hz, 2 H, 3''-H), 7.96 (s, 2 H, 5''-H), 8.13 (t, $^3J = 7.6$ Hz, 1 H, 13-H), 8.20 (d, $^3J = 8.8$ Hz, 1 H, [5' or 6']-H), 8.27 (d, $^3J = 8.8$ Hz, 1 H, [6' or 5']-H), 8.52 (dd, $^3J = 8.4$ Hz, $^4J =$

1.6 Hz, 2 H, 4''-H), 8.54 (d, $^3J = 8.4$ Hz, 1 H, 3'-H), 8.60 (dd, $^3J = 8.4$ Hz, $^4J = 1.6$ Hz, 2 H, 2''-H), 8.66 (dd, $^3J = 7.6$ Hz, $^4J = 1.2$ Hz, 1 H, 12-H), 8.97 (d, $^3J = 8.6$ Hz, 1 H, 8'-H), 9.08 (d, $^3J = 8.6$ Hz, 1 H, 7'-H) ppm. ^{13}C NMR (CD_2Cl_2 - $\text{CD}_3\text{CN} = 3:1$, 100 MHz): $\delta = 19.2, 19.3, 20.2, 20.3, 121.9, 122.7, 126.5, 128.0$ (2C), 128.1 (2C), 128.3, 128.6, 128.9, 129.4, 130.0, 130.0, 134.0, 134.2, 134.8, 135.6, 135.9, 139.1, 139.2, 140.3, 140.3, 141.3, 141.4, 142.5, 149.4, 149.6, 151.1, 151.2, 161.2, 161.6 ppm. IR (KBr): $\tilde{\nu} = 3001, 2943, 2913, 1583, 1541, 1477, 1374, 1355, 1158, 1134, 909, 862, 847, 752, 637, 629$ cm^{-1} . ESI-MS: m/z (%) 370.0 (100) $[\text{Zn}(4)(5)]^{2+}$, 888.3 (30) $[\text{Zn}(4)(5)]^+$. Anal. Calcd for $\text{C}_{49}\text{H}_{39}\text{F}_6\text{N}_5\text{O}_6\text{S}_2\text{Zn}$: C, 56.73; 3.79; N, 6.75; S, 6.18. Found: C, 56.47; 3.99; N, 6.58; S, 6.43.

Heteroleptic complex $[\text{Cu}(4)(5)](\text{ClO}_4)_2$

Compound 5 (3.45 mg, 6.99 μmol), $\text{Cu}(\text{ClO}_4)_2 \cdot 6\text{H}_2\text{O}$ (2.59 mg, 6.99 μmol) and 4 (1.26 mg, 6.99 μmol) were dissolved in CD_2Cl_2 - $\text{CD}_3\text{CN} = 3:1$ furnishing the desired complex as characterised by ESI-MS: m/z (%) 368.7 (100) $[\text{Cu}(4)(5)]^{2+}$, 836.8 (30) $[\text{Cu}(4)(5)](\text{ClO}_4)^+$.

Complex $\text{Cu}^{\text{I}}_{\text{phen}} = [\text{Cu}_2(2)(4)]^{2+}$

In an NMR tube, platform 2 (2.42 mg, 0.916 μmol), $[\text{Cu}(\text{CH}_3\text{CN})_4]\text{PF}_6$ (0.683 mg, 1.83 μmol) and ligand 4 (0.330 mg, 1.83 μmol) were dissolved in CD_2Cl_2 affording complex $\text{Cu}^{\text{I}}_{\text{phen}}$ in quantitative yield. Mp: >300 $^\circ\text{C}$. ^1H NMR (CD_2Cl_2 , 400 MHz): $\delta = 1.53$ (s, 6 H, CH_3), 1.65 (s, 12 H, CH_3), 1.66 (s, 12 H, CH_3), 1.78 (s, 12 H, CH_3), 2.12 (s, 12 H, CH_3), 2.28 (s, 12 H, CH_3), 2.30 (s, 6 H, CH_3), 2.59 (s, 12 H, CH_3), 6.00 (s, 4 H, 9-H), 6.97 (s, 4 H, 15'-H), 7.27 (dd, $^3J = 7.6$ Hz, $^4J = 1.2$ Hz, 2 H, 14-H), 7.60 (d, $^3J = 8.4$ Hz, 2 H, 4'-H), 7.71 (dd, $^3J = 8.2$ Hz, $^3J = 8.2$ Hz, 4 H, 3''-H), 7.83 (d, $^3J = 8.4$ Hz, 2 H, [4 or 7]-H), 7.86 (d, $^3J = 8.0$ Hz, 4 H, [10 or 11]-H), 7.89 (d, $^3J = 8.4$ Hz, 2 H, [7 or 4]-H), 7.91 (s, 4 H, 5', 6'-H), 7.92 (s, 4 H, 5''-H), 7.94 (t, $^3J = 7.6$ Hz, 2 H, 13-H), 7.95 (d, $^3J = 8.0$ Hz, 4 H, [16 or 17]-H), 8.12 (d, $^3J = 8.0$ Hz, 4 H, [17 or 16]-H), 8.16 (d, $^3J = 8.0$ Hz, 4 H, [11 or 10]-H), 8.21 (s, 4 H, 5-, 6-H), 8.34 (d, $^3J = 8.4$ Hz, 2 H, 3'-H), 8.36 (d, $^3J = 8.0$ Hz, 2 H, 8'-H), 8.42 (dd, $^3J = 8.2$ Hz, $^4J = 1.6$ Hz, 4 H, 4''-H), 8.45 (dd, $^3J = 8.2$ Hz, $^4J = 1.6$ Hz, 4 H, 2''-H), 8.69 (d, $^3J = 8.4$ Hz, 2 H, [3 or 8]-H), 8.70 (d, $^3J = 8.4$ Hz, 2 H, [8 or 3]-H), 8.76 (d, $^3J = 8.0$ Hz, 2 H, 7'-H), 8.77 (dd, $^3J = 7.6$ Hz, $^4J = 1.2$ Hz, 2 H, 12-H), 8.94 (d, $^3J = 4.0$ Hz, 4 H, β -H), 8.95 (d, $^3J = 4.0$ Hz, 4 H, β -H) ppm. ^{13}C NMR (CD_2Cl_2 , 100 MHz) $\delta = 19.5, 19.6, 20.2, 20.4, 20.4, 20.6, 21.2, 21.3, 94.1, 94.2, 95.7, 95.9, 105.3, 111.5, 120.3, 120.3, 120.4, 121.0, 122.8, 124.7, 124.8, 124.9, 125.1, 125.4, 126.3, 126.3, 126.4, 126.4, 126.6, 126.7, 126.9, 127.0, 127.1, 127.3, 127.4, 128.2, 128.3, 128.6, 128.6, 128.8, 129.0, 130.4, 131.5, 132.3, 134.8, 134.9, 135.0, 135.2, 135.3, 136.1, 136.2, 136.3, 136.4, 136.5, 136.7, 137.0, 137.3, 137.7, 137.7, 137.8, 138.1, 142.6, 143.2, 143.4, 144.1, 147.8, 149.1, 150.2, 150.3, 150.3, 150.3, 151.1, 151.3, 156.6, 156.6, 159.5, 159.6$ ppm. IR (KBr): $\tilde{\nu} = 2975, 2847, 2306, 2196, 1604, 1595, 1422, 1376, 1340, 1258, 1224, 1203, 1153, 1062, 1030, 850, 797$ cm^{-1} . ESI-MS: m/z (%) 1565.1 (100) $[\text{Cu}_2(2)(4)]^{2+}$. Anal. Calcd for $\text{C}_{210}\text{H}_{162}\text{Cu}_2\text{F}_{12}\text{N}_{18}\text{P}_2\text{Zn}$: C, 73.75; H, 4.77; N, 7.37. Found: C, 73.49; H, 4.87; N, 7.52.



Complex $\text{Zn}1_{\text{terpy}} = [\text{Zn}_2(2)(4)_2]^{4+}$

In an NMR tube, platform 2 (3.65 mg, 1.38 μmol), $\text{Zn}(\text{OTf})_2$ (1.00 mg, 2.76 μmol) and ligand 4 (0.498 mg, 2.76 μmol) were dissolved in $\text{CD}_2\text{Cl}_2\text{-CD}_3\text{CN} = 3:1$ furnishing complex $\text{Zn}1_{\text{terpy}}$ in quantitative yield. Mp: $>300^\circ\text{C}$. ^1H NMR ($\text{CD}_2\text{Cl}_2\text{-CD}_3\text{CN} = 3:1$, 400 MHz): $\delta = 0.94$ (s, 12 H, CH_3), 1.02 (s, 12 H, CH_3), 1.83 (s, 6 H, CH_3), 1.88 (s, 12 H, CH_3), 1.94 (s, 12 H, CH_3), 1.97 (s, 12 H, CH_3), 2.28 (s, 6 H, CH_3), 2.49 (s, 12 H, CH_3), 5.69 (s, 4 H, 15'-H), 6.91 (s, 4 H, 9-H), 7.05 (dd, $^3J = 7.6$ Hz, $^4J = 1.2$ Hz, 2 H, 14-H), 7.24 (d, $^3J = 8.4$ Hz, 2 H, 4'-H), 7.48 (d, $^3J = 8.0$ Hz, 2 H, [4 or 7]-H), 7.53 (d, $^3J = 8.0$ Hz, 2 H, [7 or 4]-H), 7.68 (dd, $^3J = 8.4$ Hz, $^4J = 8.4$ Hz, 4 H, 3''-H), 7.79 (d, $^3J = 8.0$ Hz, 4 H, [16 or 17]-H), 7.89 (s, 4 H, 5, 6-H), 7.91 (d, $^3J = 8.4$ Hz, 4 H, [10 or 11]-H), 7.92 (s, 4 H, 5''-H), 8.06 (d, $^3J = 8.4$ Hz, 4 H, [11 or 10]-H), 8.12 (d, $^3J = 8.0$ Hz, 4 H, [17 or 16]-H), 8.16 (t, $^3J = 7.6$ Hz, 2 H, 13-H), 8.19 (d, $^3J = 8.8$ Hz, 2 H, [5' or 6']-H), 8.27 (d, $^3J = 8.8$ Hz, 2 H, [6' or 5']-H), 8.33 (d, $^3J = 8.0$ Hz, 2 H, [3 or 8]-H), 8.35 (d, $^3J = 8.0$ Hz, 2 H, [8 or 3]-H), 8.51 (d, $^3J = 8.4$ Hz, 2 H, 3'-H), 8.53 (dd, $^3J = 8.4$ Hz, $^4J = 1.6$ Hz, 4 H, 4''-H), 8.62 (dd, $^3J = 8.4$ Hz, $^4J = 1.6$ Hz, 4 H, 2''-H), 8.69 (dd, $^3J = 7.6$ Hz, $^4J = 1.2$ Hz, 2 H, 12-H), 8.83 (d, $^3J = 4.8$ Hz, 4 H, β -H), 8.85 (d, $^3J = 4.8$ Hz, 4 H, β -H), 8.96 (d, $^3J = 8.4$ Hz, 1 H, 8'-H), 9.06 (d, $^3J = 8.4$ Hz, 1 H, 7'-H) ppm. ^{13}C NMR ($\text{CD}_2\text{Cl}_2\text{-CD}_3\text{CN} = 3:1$, 100 MHz) $\delta = 18.5$, 18.6, 19.0, 19.8, 20.4, 20.4, 20.6, 27.2, 93.4, 93.6, 96.1, 96.2, 105.0, 111.0, 119.4, 120.0, 122.0, 122.1, 122.5, 124.3, 124.5, 125.9, 126.2, 126.4, 126.5, 127.0, 127.0, 127.1, 127.4, 127.8, 128.0, 128.2 (2C), 128.7, 128.9, 129.2, 129.6, 129.9, 130.2, 131.7, 132.5, 133.6, 133.9, 134.2, 134.5, 135.6 (2C), 136.2 (2C), 136.4, 137.4, 137.5, 137.5, 137.6, 138.2, 139.4, 139.8, 140.0, 140.7, 140.8, 141.1, 141.5, 141.7, 142.3, 142.7, 143.5, 146.1, 148.1, 148.7, 149.5, 149.6, 149.7, 150.5, 160.0, 160.7, 161.3, 161.7 ppm. IR (KBr): $\tilde{\nu} = 2921$, 2200, 1601, 1478, 1277, 1259, 1030, 996, 797, 638 cm^{-1} . ESI-MS: m/z (%) 783.5 (50) $[\text{Zn}_2(2)-(4)_2]^{4+}$, 1094.4 (100) $[\text{Zn}_2(2)(4)_2](\text{OTf})^{3+}$, 1716.1 (20) $[\text{Zn}_2(2)(4)_2](\text{OTf})_2^{2+}$. Anal Calcd for $\text{C}_{214}\text{H}_{162}\text{F}_{12}\text{N}_{18}\text{O}_{12}\text{S}_4\text{Zn}_3\text{-CH}_2\text{Cl}_2$: C, 67.69; H, 4.33; N, 6.61; S, 3.36. Found: C, 67.56; H, 4.18; N, 6.47; S, 3.56.

Complex $\text{Cu}1_{\text{terpy}} = [\text{Cu}_2(2)(4)_2](\text{ClO}_4)_4$

Compound 2 (3.78 mg, 1.43 μmol), $\text{Cu}(\text{ClO}_4)_2 \cdot 6\text{H}_2\text{O}$ (0.530 mg, 1.43 μmol) and 4 (0.258 mg, 1.43 μmol) were dissolved in $\text{CD}_2\text{Cl}_2\text{-CD}_3\text{CN} = 3:1$ furnishing the desired complex as characterised by ESI-MS: m/z (%) 782.7 (100) $[\text{Cu}_2(2)(4)_2]^{4+}$, 1076.8 (50) $[\text{Cu}_2(2)(4)_2](\text{ClO}_4)^{3+}$.

Acknowledgements

We acknowledge generous funding by the DFG and the Universität Siegen.

Notes and references

- (a) L. B. Jilaveanu, C. R. Zito and D. Oliver, *Proc. Natl. Acad. Sci. U. S. A.*, 2005, **102**, 7511; (b) M. Schliwa and

- G. Woehlke, *Nature*, 2003, **422**, 759; (c) M. A. Geeves and K. C. Holmes, *Annu. Rev. Biochem.*, 1999, **68**, 687.
- (a) S. J. Cantrill, A. R. Pease and J. F. Stoddart, *J. Chem. Soc., Dalton Trans.*, 2000, 3715; (b) T. Murahashi, K. Shirato, A. Fukushima, K. Takase, T. Suenobu, S. Fukuzumi, S. Ogoshi and H. Kurosawa, *Nat. Chem.*, 2012, **4**, 52; (c) C. Wang, Z. Li, D. Cao, Y.-L. Zhao, J. W. Gaines, O. A. Bozdemir, M. W. Ambrogio, M. Frascioni, Y. Y. Botros, J. I. Zink and J. F. Stoddart, *Angew. Chem., Int. Ed.*, 2012, **51**, 5460.
- (a) J.-P. Sauvage, *Acc. Chem. Res.*, 1998, **31**, 611; (b) A. M. Brouwer, C. Frochot, F. G. Gatti, D. A. Leigh, L. Mottier, F. Paolucci, S. Roffia and G. W. H. Worpel, *Science*, 2001, **291**, 2124; (c) V. Amendola, L. Fabbrizzi, C. Mangano and P. Pallavicini, *Acc. Chem. Res.*, 2001, **34**, 488; (d) Y. Liu, A. H. Flood, P. A. Bonvallet, S. A. Vignon, B. H. Northrop, H.-R. Tseng, J. A. Jeppesen, T. J. Huang, B. Brough, M. Baller, S. Magonov, S. D. Solares, W. A. Goddard, C.-M. Ho and J. F. Stoddart, *J. Am. Chem. Soc.*, 2005, **127**, 9745; (e) B. Colasson, N. L. Paul, Y. L. Mest and O. Reinaud, *J. Am. Chem. Soc.*, 2010, **132**, 4393.
- V. Balzani, A. Credi and M. Venturi, *Molecular Devices and Machines*, Wiley-VCH, Weinheim, 2nd edn, 2008; B. L. Feringa and W. R. Browne, *Molecular Switches 1+2*, Wiley-VCH, Weinheim, 2nd edn, 2011.
- (a) J.-P. Collin, C. Dietrich-Buchecker, P. Gavina, M. C. Jimenez-Molero and J.-P. Sauvage, *Acc. Chem. Res.*, 2001, **34**, 477; (b) J. D. Badjic, C. M. Ronconi, J. F. Stoddart, V. Balzani, S. Silvi and A. Credi, *J. Am. Chem. Soc.*, 2006, **128**, 1489; (c) T. Song and H. Liang, *J. Am. Chem. Soc.*, 2012, **134**, 10803; (d) B. Lewandowski, G. D. Bo, J. W. Ward, M. Pappmeyer, S. Kuschel, M. J. Aldegunde, P. M. E. Gramlich, D. Heckmann, S. M. Goldup, D. M. D'souza, A. E. Fernandes and D. A. Leigh, *Science*, 2013, **339**, 189.
- (a) R. T. Kelly, H. De Silva and R. A. Silva, *Nature*, 1999, **401**, 150; (b) M. C. Jiménez, C. Dietrich-Buchecker and J.-P. Sauvage, *Angew. Chem., Int. Ed.*, 2000, **39**, 3284; (c) M. Haga, T. Takasugi, A. Tomie, M. Ishizuya, T. Yamada, M. D. Hossain and M. Inoue, *Dalton Trans.*, 2003, 2069; (d) M. Alvarez-Pérez, S. M. Goldup, D. A. Leigh and A. M. Z. Slawin, *J. Am. Chem. Soc.*, 2008, **130**, 1836; (e) G. Haberhauer, *Angew. Chem., Int. Ed.*, 2010, **49**, 9286; (f) S. K. Samanta and M. Schmittel, *J. Am. Chem. Soc.*, 2013, **135**, 18794.
- (a) N. Armaroli, V. Balzani, J.-P. Collin, P. Gaviña, J.-P. Sauvage and B. Ventura, *J. Am. Chem. Soc.*, 1999, **121**, 4397; (b) A. Carella, C. Coudret, G. Guirado, G. Rapenne, G. Vives and J.-P. Launay, *Dalton Trans.*, 2007, 177; (c) F. Durola and J.-P. Sauvage, *Angew. Chem., Int. Ed.*, 2007, **46**, 3537; (d) Y.-L. Zhao, W. R. Dichtel, A. Trabolsi, S. Saha, I. Aprahamian and J. F. Stoddart, *J. Am. Chem. Soc.*, 2008, **130**, 11294; (e) L. Fang, C. Wang, A. C. Fahrenbach, A. Trabolsi, Y. Y. Botros and J. F. Stoddart, *Angew. Chem., Int. Ed.*, 2011, **50**, 1805; (f) T. Avellini, H. Li, A. Coskun, G. Barin, A. Trabolsi, A. N. Basuray, S. K. Dey, A. Credi,



- S. Silvi, J. F. Stoddart and M. Venturi, *Angew. Chem., Int. Ed.*, 2012, **51**, 1611; (g) M. Nishikawa, S. Kume and H. Nishihara, *Phys. Chem. Chem. Phys.*, 2013, **15**, 10549.
- 8 (a) N. Koumura, R. W. J. Zijlstra, R. A. van Delden, N. Harada and B. L. Feringa, *Nature*, 1999, **401**, 152; (b) T. Muraoka, K. Kinbara, Y. Kobayashi and T. Aida, *J. Am. Chem. Soc.*, 2003, **125**, 5612; (c) T. Muraoka, K. Kinbara and T. Aida, *Nature*, 2006, **440**, 512; (d) S. Kume and H. Nishihara, *Dalton Trans.*, 2008, 3260; (e) A. Coskun, D. C. Friedman, H. Li, K. Patel, H. A. Khatib and J. F. Stoddart, *J. Am. Chem. Soc.*, 2009, **131**, 2493; (f) M. C. Basheer, Y. Oka, M. Mathews and N. Tamaoki, *Chem. – Eur. J.*, 2010, **16**, 3489; (g) Z. Li, J. Liang, W. Xue, G. Liu, S. H. Liu and J. Yin, *Supramol. Chem.*, 2014, **26**, 54.
- 9 (a) A. Livoreil, C. O. Dietrich-Buchecker and J.-P. Sauvage, *J. Am. Chem. Soc.*, 1994, **116**, 9399; (b) J. P. Collin, F. Durola, J. Lux and J.-P. Sauvage, *Angew. Chem., Int. Ed.*, 2009, **48**, 8532; (c) H. Li, A. C. Fahrenbach, A. Coskun, Z. Zhu, G. Barin, Y.-L. Zhao, Y. Y. Botros, J.-P. Sauvage and J. F. Stoddart, *Angew. Chem., Int. Ed.*, 2011, **50**, 6782.
- 10 M. L. Saha, S. Neogi and M. Schmittel, *Dalton Trans.*, 2014, **43**, 3815.
- 11 (a) H. Sleiman, P. Baxter, J.-M. Lehn and K. Rissanen, *J. Chem. Soc., Chem. Commun.*, 1995, 715; (b) J. Frey, C. Tock, J.-P. Collin, V. Heitz, J.-P. Sauvage and K. Rissanen, *J. Am. Chem. Soc.*, 2008, **130**, 11013; (c) S. Durot, F. Reviriego and J.-P. Sauvage, *Dalton Trans.*, 2010, **39**, 10557; (d) R. S. Forgan, J.-P. Sauvage and J. F. Stoddart, *Chem. Rev.*, 2011, **111**, 5434.
- 12 (a) M. Schmittel and A. Ganz, *Chem. Commun.*, 1997, 999; (b) M. Schmittel, U. Lüning, M. Meder, A. Ganz, C. Michel and M. Herderich, *Heterocycl. Commun.*, 1997, **3**, 493; (c) M. Schmittel, V. Kalsani, R. S. K. Kishore, H. Cölfen and J. W. Bats, *J. Am. Chem. Soc.*, 2005, **127**, 11544; (d) M. Schmittel and S. K. Samanta, *J. Org. Chem.*, 2010, **75**, 5911; (e) S. De, K. Mahata and M. Schmittel, *Chem. Soc. Rev.*, 2010, **39**, 1555.
- 13 (a) M. M. Safont-Sempere, G. Fernández and F. Würthner, *Chem. Rev.*, 2011, **111**, 5784; (b) K. Osowska and O. Š. Miljanić, *Synlett*, 2011, 1643; (c) M. L. Saha and M. Schmittel, *Org. Biomol. Chem.*, 2012, **10**, 4651; (d) S. Saha and P. Ghosh, *J. Chem. Sci.*, 2012, **124**, 1229.
- 14 (a) K. Parimal, E. H. Witlicki and A. H. Flood, *Angew. Chem., Int. Ed.*, 2010, **49**, 4628; (b) K. Osowska and O. Š. Miljanić, *J. Am. Chem. Soc.*, 2011, **133**, 724; (c) A.-M. Stadler, C. Burg, J. Ramírez and J.-M. Lehn, *Chem. Commun.*, 2013, **49**, 5733.
- 15 (a) DFT computations were performed with the B3LYP functional, 6-31G* basis set for all main group elements and LANL2DZ basis set for copper implemented in Gaussian 09; (b) M. J. Frisch, *et al.*, *Gaussian 09, Revision B.01*.
- 16 In parenthesis, the relative energies are given with respect to the lowest energy structure. Structures iso-**I**^C and iso-**III** could not be optimised in DFT computations due to severe steric crowding between the mesityl groups.
- 17 In another experiment when **3** and **5** were mixed with Cu⁺ or Zn²⁺ at a 1 : 1 : 1 ratio, there was no evidence for the formation of the heteroleptic species neither by ¹H NMR nor ESI-MS.

